Nucleation of carbon clusters

Xiaodun Jing and James R. Chelikowsky
Department of Chemical Engineering and Materials Science, Minnesota Supercomputer Institute, University of Minnesota, Minneapolis, Minnesota 55455
(Received 21 August 1992)

The growth of carbon clusters by monomer addition, at constant temperature, is examined via Langevin molecular-dynamics simulations by using a recently developed many-body interatomic potential for carbon. The simulations are performed at temperatures below the melting point of graphite. We find for carbon clusters with fewer than ~20 atoms that "ringlike" structures are the dominant species present. "Spheroidal" structures dominate for larger clusters of sizes above ~30 atoms. It is found that carbon monomers form bonds at the surface of the spheroidal cluster during the process of cluster growth. No monomer is found to be captured inside the hollow of a spheroidal cluster during the simulation. A subunit of one pentagonal ring surrounded by five hexagonal rings in the cluster is found to appear frequently for clusters of sizes larger than ~40 atoms. This structure can be thought of as a precursor for the formation of the C_{60} fullerene.

I. INTRODUCTION

Understanding of the formation process of C_{60} has remained a fundamental issue since its discovery.[1-6] Each atom is in an equivalent position in the C_{60} molecule. It is hard to envisage a precise mechanism by which such a large, highly symmetric molecule could be formed. Some pioneering work on the formation of the C_{60} molecule has been performed. For example, simulated annealing of carbon clusters[4] has suggested that the low-energy structures are hollow spheroids in the size range $50 \leq n \leq 72$. Many calculations with symmetry restrictions[7-10] have been done for the single C_{60} molecule. These calculations agree with the measured bond lengths and binding energy. Also, one simulation[6] has obtained a fullerenelike structure for C_{60} by the direct nucleation of 60 carbon atoms from a "hot carbon plasma." However, the specific details of the formation process of C_{60} remain unsolved.

Smalley[5] proposed that during the process of graphite sheet formation, some atoms form into pentagonal rings instead of hexagonal rings. The pentagons cause the bending of the sheet. The further growth and formation of pentagons and hexagons would ultimately cause the molecule to close. However, it is unlikely that fullerenes are formed directly by the folding of graphitelike sheets. Recent experiments using C^{12}/C^{13} isotope scrambling measurements[11] have shown that C_{60} is formed in an "atomic-carbon" vapor environment; the starting point for the formation process is a monomer, or a very small cluster. Hence, the simulation for the nucleation of C_{60} from the gas phase[6,12,13] is a reasonable model for the formation of C_{60}. In order to simulate the growth process of carbon clusters, we have carried out a systematic molecular-dynamics (MD) study starting from a very small cluster with only a few atoms, and examining its growth through monomer addition.

The interatomic potential used in the dynamic simulation and the details of Langevin molecular-dynamic simulation are given in Sec. II. The results and discussions are presented in Sec. III, and a brief summary and conclusions are given in Sec. IV.

II. LANGEVIN MOLECULAR-DYNAMICS SIMULATIONS

The interatomic potential used in our simulation is the same as the potential used in the previous simulations.[6,12-14] The full description of the potential is given in Ref. 12. Here, we give only the essential features of this potential. Unlike a closed-shell system, which does not involve covalent chemical bond formation, the use of bonding forces determined from an interatomic potential for a system with open-shell species is nontrivial. The potentials for covalent bonding are directional, and depend strongly on the local environment. Also, the potentials should take into account "over-coordinated" and "under-coordinated" effects.

Our interatomic potential for carbon incorporates such features, and yields accurate binding energies and bond lengths for carbon in the diamond and graphite structures. The data for the diamond structure are the following: cohesive energy 7.28 eV per atom and bond length 3.53 Å, compared with experimental data 7.37 eV per atom[15] and 3.57 Å.[16] For graphite structure, the cohesive energy is 7.33 eV per atom and lattice constants are $a_0=2.51$ Å, $c_0=6.17$ Å, compared with the experimental data, cohesive energy 7.41 eV/ atom[17] and lattice constants $a_0=2.45$ Å, $c_0=6.67$ Å.[18] For dense forms of carbon, such as face-centered-cubic carbon, we obtain reasonably accurate agreement with *ab initio* pseudopotential calculations.[12] The largest error for graphite results from the neglect of the van der Waals character of the interplanar interactions.

We obtain reasonably accurate structure parameters for the ideal C_{60} fullerene. The calculated cohesive energy and bond lengths are 7.03 eV per atom, 1.34 and 1.57 Å, respectively. The experimental bond lengths are 1.40

and 1.47 Å,[19] respectively. From *ab initio* pseudopotential calculations the cohesive energy of the C_{60} fullerene is estimated to be ~ 7.0 eV.[20]

Langevin molecular dynamics[12,21] is used in this simulation. In this approach, particles are considered to move in a viscous medium and experience a rapidly fluctuating random force $\mathbf{G}(t,T)$, which is a function of time t and temperature T. The equations of motion for a specific particle are

$$\frac{\partial \mathbf{r}}{\partial t}=\mathbf{v}\ ,$$
$$m\frac{\partial \mathbf{v}}{\partial t}=\mathbf{F}-\gamma\mathbf{v}+\mathbf{G}(t,T)\ , \tag{1}$$

where $\mathbf{F}$ is the force arising from other particles in the system, and γ is the viscosity coefficient. m and $\mathbf{v}$ are the mass and velocity of the particle, respectively. The random force has a mean of zero. The correlation function is given by

$$\langle G_i(t,T)G_i(t',T)\rangle = 2\gamma k_B T\delta(t-t')\ . \tag{2}$$

The viscosity coefficient in (2) ensures that the random force performs as much work on the particle as is dissipated by the viscous friction. In an equilibrium state, the mean kinetic energy of the particle is related to the temperature of the system T by the equipartition relation

$$\langle \tfrac{1}{2}mv^2\rangle_{\rm eq}=\tfrac{3}{2}k_B T\ . \tag{3}$$

Thus, the random fluctuating force simulates an isothermal bath with temperature T. This thermal fluctuating force drives the system to equilibrium which is characterized by the temperature.

This method has several advantages over other simulation techniques. Since the total energy is not conserved, much larger time steps are generally possible with this method than with the microcanonical MD method, allowing simulations over longer times. The temperature of the heat bath can be directly specified, and controlled, which is more easily adaptable for numerical simulations as compared with the microcanonical MD. The thermal bath has a "physical" analogy to the real system. The viscous medium can be thought of as the buffer gas in which the C_{60} molecules are nucleated. As with other simulation methods, the disadvantage of this method is the short time span which can be followed. Nonetheless, we can obtain insights into the types of structures which are likely to form rapidly, and how these structures might lead to the formation of an ideal C_{60} fullerene.

By using the interatomic potential and Langevin MD simulation discussed above, we simulate the growth process of carbon clusters at a fixed temperature. The growth process is simulated by adding carbon monomers to an existing carbon cluster one after another. The simulation is contained in a sphere, and its size is always kept large enough not to bias the growth process of the cluster. We monitor the rate of carbon atoms hitting the spherical boundary. This rate is taken to be less than one per thousand time steps. For an atom hitting the boundary, reflecting boundary conditions are used, i.e., when a carbon atom hits the spherical boundary, its velocity is reversed in direction. The initial position of the added monomer is taken randomly on the spherical boundary, the velocity direction of the monomer is taken toward the center of the sphere, its speed satisfies the Maxwell distribution for the simulation temperature. The simulation time step is $\delta t = 80$ a.u. (1 a.u. $=2.42\times10^{-17}$ sec), which corresponds to ~ 2 fsec. The vibration periods of the carbon atom in the ideal C_{60} molecule are of the order of ~ 100 fsec by using our potential,[22] which is the same order of magnitude as the experimental data.[23] The simulation time step is much smaller than the vibration period of the carbon atom in the C_{60} molecule. The viscosity $\gamma=0.002$ in a.u. and $\gamma\delta t=0.16$ is less than 1 as required by the stability of the simulation. The initial configuration is taken to be a sixfold ring, which is energetically favorable with our potential. Our simulations indicate that the morphology of large clusters has only a weak dependence on the initial configuration. The most likely errors introduced in our model are the introduction of defect structures which cannot be annealed out in the short time frame of the theoretical simulations.

III. RESULTS AND DISCUSSIONS

Simulations were done at two different temperatures, $T=2000$ and 4500 K. We chose the low temperature to correspond to typical growth conditions, and the high temperature to be near the melting point of graphite, which is approximately $\sim 4000-5000$ K.[24] These temperatures will ensure cluster stability as we follow its growth. A temperature which is too high will inhibit the cluster growth as "hot" carbon atoms may escape the cluster. Conversely, at a temperature which is too low, the cluster will "freeze" prematurely into a metastable configuration. The total number of integration steps for each monomer cycle is generally determined by the time needed for the monomer to be bonded to the existing cluster. The average number of steps for each monomer cycle is about 3000, which corresponds to 6 psec.

At $T=2000$ K, if we generate the initial configuration by putting the six atoms randomly in the sphere, this configuration will evolve quickly to a sixfold ring. As monomers are added into the system, it is found that in most cases one "big ring" which contains more than six atoms is formed. As additional monomers are added to the system, branches are formed across the "big ring." A typical structure for a cluster of size $n=11$ is shown in Fig. 1(a). The cluster tends to take the form of an annular ring when it grows to the size about 20 atoms. A typical configuration for this cluster size is given in Fig. 1(b). A "spheroidal" structure with polycyclic rings on the surface is formed when the cluster contains ~ 30 atoms. In Fig. 1(c), we give one of the structures of size $n=32$.

For clusters with $n \gtrsim 25$, monomers move from spherical boundary to the surface of the "spheroidal" cluster and form bonds with other atoms on the surface at what may be called "defect regions," i.e., regions in the cluster where some atoms are bonded to less than three atoms. Because of the "spheroidal" or "imperfect" fullerene structure, the monomer can be easily bonded at the surface, but it has much less chance to be captured inside the cage.

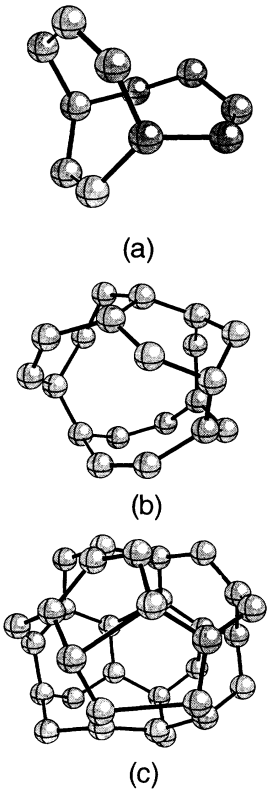

FIG. 1. Some typical structures for different sizes of carbon clusters at $T=2000$ K. (a) $n=11$, (b) $n=20$, (c) $n=32$.

In order to examine more clearly the formation process, we have calculated the average percentage of twofold-coordinated atoms and threefold-coordinated atoms as a function of cluster size n. The bond length cutoff is chosen to be 1.9 Å; this distance is shorter than the second-nearest-neighbor separation, and is large enough to avoid fluctuations of the coordination number for each atom. The results are shown in Fig. 2. The data are obtained from the average of several independent runs. Twofold-coordinated atoms represent a "ringlike" environment and threefold-coordinated atoms represent a "fullerenelike" environment. From the plot in Fig. 2, we

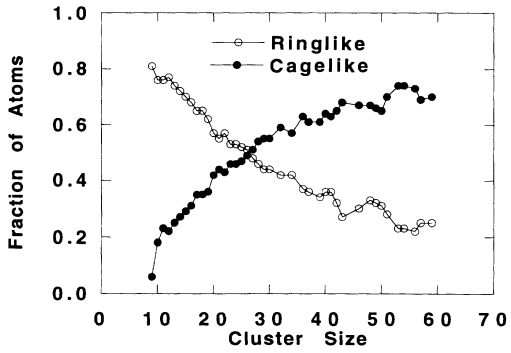

FIG. 2. The fraction of carbon atoms in ringlike sites (twofold-coordinated sites) and cagelike sites (threefold-coordinated sites) as a function of cluster size. As carbon clusters grow via monomer addition, ringlike sites dominate small clusters, but above ~30 atoms cagelike sites dominate.

can see that the cluster morphology changes from ringlike structures to fullerenelike structures as the cluster grows. The steep increase of threefold-coordinated atoms at cluster size around $n=20$ is the indication of the formation of an annular ring structure. When the cluster grows to the size between 25 and 30, threefold-coordinated atoms exceed twofold-coordinated atoms. This corresponds to the formation of a "spheroidal" structure. The "spheroidal" structure is further verified by the radial distribution of carbon atoms in the cluster. We chose the mass center of the cluster as the origin of the radial distribution function. The distribution function gives the number of atoms between R and $R+\Delta R$ from the origin. The normalized distribution function is plotted versus R in Fig. 3(a). The peak position gives the "radius" of the cluster. The narrow peak indicates a "spheroidal" structure of the cluster. The radius for $n=60$ is approximately 4.0 Å, which is about the radius of a C_{60} molecule.[25]

One important feature of our simulations is that no atom is captured inside the cluster for the growth rate about 6 psec per atom. For a fast growth rate (about 1 psec per atom), we did find atoms inside, but in this configuration the "spheroidal" structure is unstable. The resulting clusters are similar to "amorphous" carbon clusters as there exist some fourfold-coordinated atoms within the cluster.

Some unusually stable spheroidal clusters can be observed during our simulation process from the large binding energies, and the longer time needed for the added monomers to be bonded to the existing cluster. These stable clusters contain, 20, 32, 36, 48, etc. atoms. This is consistent with the experimental results,[2,26,27] and the "magic numbers" proposed by Kroto.[28]

To examine the temperature dependence of cluster growth, a second simulation was performed at $T=4500$ K. We get the same qualitative results as $T=2000$ K. Because of the entropy effect, clusters assume more open structures at higher temperatures. The spheroidal structure is formed at slightly larger cluster sizes. The radial distributions for several different sizes of clusters are given in Fig. 3(b), and the "spheroidal" structure is seen clearly from this plot. Our simulations at these temperatures show a strong onset of sixfold rings at cluster sizes $n\sim 30$. This onset indicates the formation of "spheroidal" structures.

Compared to the case $T=2000$ K, the growth rate to form a "spheroidal" structure at $T=4500$ K is much faster. At higher temperatures, it is easier to transform one local configuration to a more stable one. At lower temperatures, once a monomer is bonded to the cluster, it is difficult for this monomer to overcome the energy barrier to form a more stable local configuration. This is the reason for the existence of small peaks in the radial distributions at $T=2000$ K. But at high temperatures, the clusters contain large numbers of low coordinated atoms. This trend also hinders the onset of "spheroidal" structures.

To investigate the annealing effect, we have performed an annealing simulation for a cluster of 36 atoms from temperature 4500 to 1500 K by using a logarithm anneal-

ing schedule. The total annealing time is about 40 psec. The radial distributions at different temperatures are shown in Fig. 4. It can be seen that the width of this distribution decreases from about 2 Å at 4500 K to less than 1 Å at 1500 K. The binding energy per atom of the cluster increases from 5.76 to 6.44 eV. During the annealing,

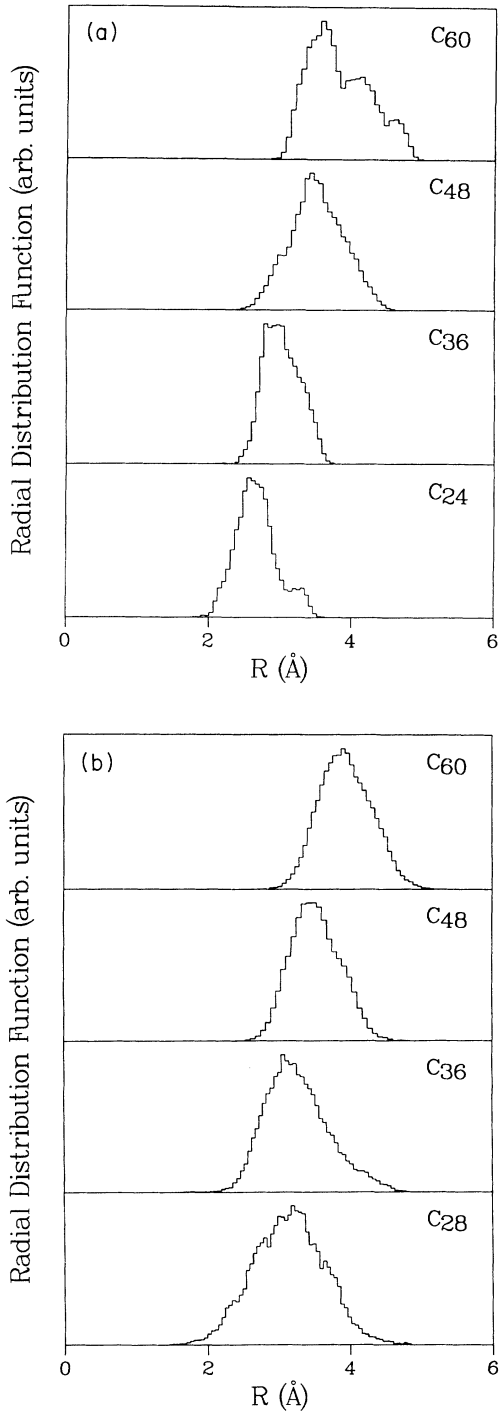

FIG. 3. The radial distribution functions for carbon clusters of different sizes as indicated in the figures at two different temperatures. The origin of the radial distribution function is chosen to be the center of mass of the corresponding cluster. (a) $T=2000$ K, $n=24,36,48,60$. (b) $T=4500$ K, $n=28,36,48,60$.

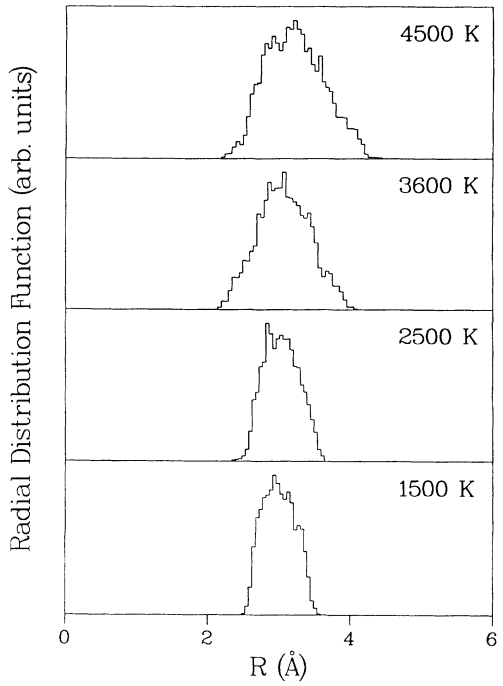

FIG. 4. The radial distribution functions for carbon clusters C_{36} at different temperatures.

the structure of the cluster is very stable for temperatures below 2500 K as contrasted to temperatures above 2500 K. From this observation, we estimate that an "optimal" temperature for the nucleation of fullerene carbon cluster is around 2000–3000 K.

Since pentagonal rings are energetically unfavorable compared to hexagonal rings, they can be easily broken once formed. This is reflected in our simulations from the fact that the number of pentagons is much smaller than that of hexagons, and the relative fluctuation of the number of pentagons is much larger than that of hexagons. However, if a pentagon is surrounded by five or even four hexagons, the pentagonal ring becomes very stable. Such a pentagonal ring structure is found frequently during our simulations for cluster size above 40 atoms, but is infrequently observed for smaller clusters. The formation of this structure in smaller clusters produces more dangling bonds instead of reducing the number. Figure 5 illustrates one of the clusters which contains this pentagonal structure. The stability of this pentagonal subunit promotes the nucleation of the "perfect" fullerene structure. In this sense, the pentagonal ring subunit can be viewed as a "precursor" to the formation of C_{60}.[5,29]

To examine the stability of this "precursor" structure, we have calculated the cohesive energies of C_{20} clusters with a perfect cap structure[29,30] and a perfect cage structure[29] as shown in Figs. 6(a) and 6(b). The cohesive energies are 5.8 and 5.66 eV, respectively. Both these cohesive energies are smaller than that of the structure obtained by MD simulation in Fig. 1(b) of cohesive energy 5.89 eV. Considering the high symmetry and the low cohesive energy, the chance for C_{20} clusters to form ei-

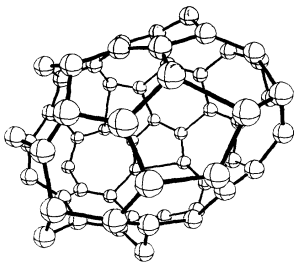

FIG. 5. A C_{60} cluster showing the pentagonal subunit, i.e., a pentagonal ring surrounded by five hexagonal rings. This subunit is an important precursor in the formation of C_{60} fullerene.

ther the perfect cap structure as in Fig. 6(a), or the perfect cage structure as in Fig. 6(b), is expected to be very small. In the process of our MD simulation, we sometimes observed "bowl"-shaped structures with much less symmetry than the cap structure of Fig. 6(a) for cluster size around 20 atoms at $T=2000$ K. But when the cluster grows to the size about 30 atoms, it tends to close and form a "spheroidal" structure with many "defects" on the surface.

Owing to the fast annealing, many defects exist in C_{60} clusters in our simulations relative to the ideal C_{60} molecule. The cohesive energy of the structure in Fig. 5 is ~ 6.5 eV, which is less than that of an ideal C_{60} molecule, ~ 7.0 eV. We find that by repeated anneals, the cohesive energy will increase to almost 6.8 eV. However, certain defects, such as adjacent fivefold rings, are difficult to remove even with the longest annealing times which are feasible, e.g., ~ 1 ns. We estimate the energy difference between an ideal C_{60} and one with one pair of adjacent fivefold rings to be approximately ~ 1 eV. This value is consistent with estimates made from quantum chemistry calculations.[31] But the activation barrier for the above defect is estimated to be above 5 eV. It has been suggested that the energy released by monomer, or dimer, addition can promote the removal of such defects.[32] One might speculate that such defects are annealed out early in the growth process of the C_{60} molecule; otherwise, such defects would likely remain in the larger clusters. In this manner, one might avoid the creation of defects with large activation barriers relative to the ideal structure. It is observed that in our simulations the configurations of the clusters change more easily during the monomer addition process than a simulation process with a constant number of atoms.

It should be possible to investigate other forms of carbon with our potential. For example, it may be possible to study the formation of amorphous carbon[33] by quick annealing, just as found in our simulation. If we use a higher growth rate, the resulting clusters have structures similar to an amorphous carbon cluster with a higher coordination number than the hollow spheroidal structure.

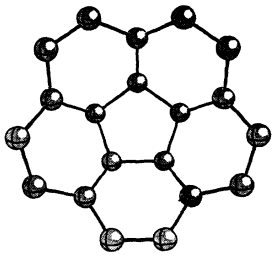

(a)

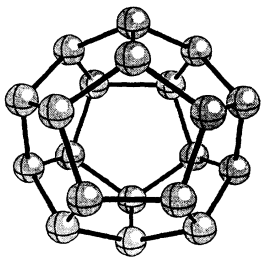

(b)

FIG. 6. Different structures of C_{20} clusters. (a) A perfect cap structure. (b) A perfect cage structure.

IV. CONCLUSIONS

In conclusion, our molecular-dynamics simulations give qualitative insights to the formation of carbon fullerenes. The formation of clusters with "fullerenelike" structures can be simulated from an "atomic-carbon" vapor environment under suitable temperatures. Our work is consistent with the recent isotope scrambling experiment.[11] We find "spheroidal" structures start to form when the cluster size is about between 20–30 atoms at 2000 K. We estimate the optimal temperature for the formation of fullerene structure to be around 2000–3000 K. The formation of imperfect fullerene structures increases the possibility of surface bond formation, and prevents the capture of carbon atoms inside the hollow of the cluster. The appearance of a "precursor structure," i.e., a pentagonal ring surrounded by hexagonal rings, in clusters with $n \gtrsim 40$ aids the formation of perfect fullerene structures.

ACKNOWLEDGMENTS

Acknowledgment is made to the Donors of The Petroleum Research Fund, administrated by the American Chemical Society, and Exxon Research and Engineering Company for support of this research. We would like to acknowledge computational support from the Minnesota Supercomputer Institute. We would also like to thank Keith Glassford for helpful discussions.

[1]H. W. Kroto, J. R. Heath, S. C. O'Brein, R. F. Curl, and R. E. Smalley, Nature (London) **318**, 162 (1985).
[2]R. F. Curl and R. E. Smalley, Science **242**, 1017 (1988).
[3]H. W. Kroto and K. McKay, Nature (London) **331**, 328 (1988); H. W. Kroto, Pure Appl. Chem. **62**, 407 (1990).
[4]P. Ballone and P. Milani, Phys. Rev. B **42**, 3201 (1990).
[5]R. E. Smalley, The Sciences **31**, 22 (1991).
[6]J. R. Chelikowsky, Phys. Rev. Lett. **67**, 2970 (1991).
[7]D. S. Marynick and S. Estreicher, Chem. Phys. Lett. **132**, 383 (1986).
[8]S. Satpathy, Chem. Phys. Lett. **130**, 545 (1986).
[9]M. L. McKee and W. C. Herndon, J. Mol. Struct. (THEOCHEM.) **153**, 75 (1987).
[10]B. I. Dunlap, Int. J. Quantum Chem., Quantum Chem. Symp. **22**, 257 (1988).
[11]T. W. Ebbesen, J. Tabuchi, and K. Tanigaki, Chem. Phys. Lett. **191**, 336 (1992).
[12]J. R. Chelikowsky, Phys. Rev. B **45**, 12 062 (1992).
[13]X. Jing and J. R. Chelikowsky, Phys. Rev. B **46**, 5028 (1992).
[14]J. R. Chelikowsky and J. C. Phillips, Phys. Rev. B **41**, 5735 (1990); J. R. Chelikowsky, K. M. Glassford, and J. C. Phillips, *ibid.* **44**, 1538 (1991).
[15]L. Brewer (unpublished).
[16]J. Donohue, *The Structure of the Elements* (Wiley, New York, 1974).
[17]N. N. Greenwood and A. Earnshaw, *Chemistry of the Elements* (Pergamon, Oxford, 1984).
[18]Y. Baskin and L. Mayer, Phys. Rev. **100**, 544 (1955).
[19]W. Kratschmer, L. D. Lamb, K. Fostiropoulos, and D. R. Huffman, Nature (London) **347**, 354 (1990).
[20]N. Troullier and J. L. Martins, Phys. Rev. B **46**, 1754 (1992).
[21]R. Biswas and D. R. Hamann, Phys. Rev. B **34**, 895 (1986).
[22]Ramesh Kizhappali (private communication).
[23]R. L. Cappelletti, J. R. D. Copley, W. A. Kamitakahara, Fang Li, J. S. Lannin, and D. Ramage, Phys. Rev. Lett. **66**, 3261 (1991).
[24]G. Galli, R. M. Martin, R. Car, and M. Parrinello, Science **250**, 1547 (1990).
[25]Q.-M. Zhang, Jae-Yel Yi, and J. Bernholc, Phys. Rev. Lett. **66**, 2633 (1991).
[26]Q. L. Zhang, S. C. O'Brein, J. R. Heath, Y. Liu, R. F. Curl, H. W. Kroto, and R. E. Smalley, J. Phys. Chem. **90**, 525 (1986).
[27]H. W. Kroto, J. R. Heath, S. C. O'Brein, R. F. Curl, and R. E. Smalley, Nature (London) **318**, 162 (1985).
[28]H. W. Kroto, Nature (London) **329**, 529 (1987).
[29]C. J. Brabec, E. Anderson, B. N. Davidson, S. A. Kajihara, Q-M Zhang, J. Bernholc, and D. Tomanek, Phys. Rev. B **46**, 7326 (1992).
[30]A. D. J. Haymet, J. Am. Chem. Soc. **108**, 319 (1986).
[31]K. Raghavachari and C. M. Rohlfing, J. Phys. Chem. **96**, 2463 (1992).
[32]J. Y. Yi and J. Bernholc (unpublished).
[33]G. Galli, Richard M. Martin, R. Car, and M. Parrinello, Phys. Rev. B **42**, 7470 (1990).

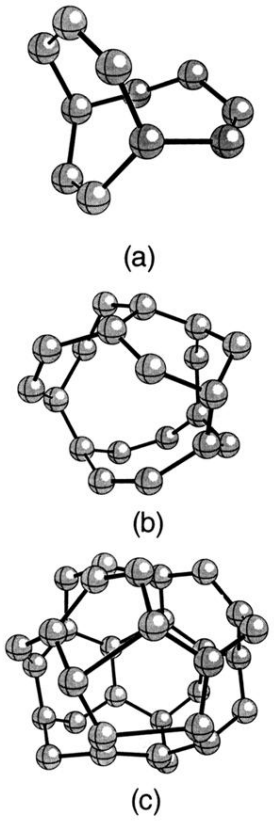

FIG. 1. Some typical structures for different sizes of carbon clusters at $T=2000$ K. (a) $n=11$, (b) $n=20$, (c) $n=32$.

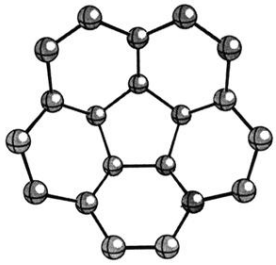

(a)

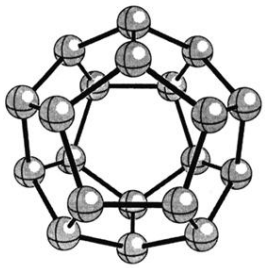

(b)

FIG. 6. Different structures of C_{20} clusters. (a) A perfect cap structure. (b) A perfect cage structure.